Thermal, Mechanical, and Dielectric Properties of Polystyrene/Expanded Graphite Nanocomposites

R. K. Goyal,[1]* P. A. Jagadale,[2] U. P. Mulik[1]

[1]*Centre for Materials for Electronics Technology, Govt. of India, Panchwati, Pune 411008, India*
[2]*Department of Chemistry, Annasaheb Magar College, Hadapsar, Pune 411028, India*

Received 16 October 2007; accepted 7 July 2008
DOI 10.1002/app.29042
Published online 10 November 2008 in Wiley InterScience (www.interscience.wiley.com).

ABSTRACT: We herewith report the thermal, mechanical (modulus), and dielectric properties of polystyrene (PS)/expanded graphite (EG) nanocomposites fabricated by a simple technique of dispersing EG (up to 2.5 vol %) in PS matrix via solution method followed by hot pressing. The thermal stability and char yield of the nanocomposites are improved marginally. The modulus, electrical conductivity, dielectric constant, and dielectric loss tangent of the nanocomposites are significantly increased with EG content. The modulus of the nanocomposites increases by about twofold at 30°C compared with that of pure PS. The dielectric constant and the loss tangent of nanocomposites are increased up to 13-fold and 200-fold compared with that of pure PS, respectively, at 1 MHz and varied with frequency. © 2008 Wiley Periodicals, Inc. J Appl Polym Sci 111: 2071–2077, 2009

Key words: nanocomposite; conductivity; modulus; dielectric constant; loss tangent

INTRODUCTION

To synthesize electrically conducting polymers, loading of electrically conductive microsized particles must be as high as 10 vol % or even higher.[1,2] The high particle loading results in a material with relatively high density, poor mechanical, and optical properties[3] compared with composites containing low particle loading. In view of this, development of polymer nanocomposite containing conducting nanoparticles has been extensively investigated. The nanoparticles usage results in significant improvement in thermal, mechanical, and electrical properties of polymers even with very low loading levels compared with microparticles.[4] Nevertheless, nanocomposite properties depend strongly on size, shape, aggregate size, surface characteristics, and degree of dispersion of the nanoparticles. To improve the properties, a homogeneous dispersion of the nanoparticles in the polymer matrix is essential.

Recently, expanded graphite (EG) has been widely used as electrically conductive filler for electrically conductive polymer composites due to its attractive properties such as high aspect ratio (100–500) than that of natural graphite flake or powder resulting easy dispersion into polymer matrix.[3] Moreover, presence of multipores, functional carboxyl and hydroxyl groups on the EG surface facilitates physical and chemical adsorption between the EG and the polymer molecule.[5,6] The EG filled polymer nanocomposites have been synthesized by various techniques viz. mechanical mixing, melt mixing, and *in situ* polymerization methods and have shown many potential applications, e.g., electromagnetic interference (EMI) shielding of computers and electronic equipments, electrode materials, conductive adhesive for electronics packaging, flip-chips, cold solders, static charge dissipating materials, cathode ray tubes and fuel cells, corrosion resistant and radar absorbent coating, and switching devices.[4,7,8]

Recently, several researchers have reported electrical properties of poly(methyl methacrylate)/EG,[5] Nylon 6/EG,[9] and polystyrene (PS)/EG[10] nanocomposites. Xiao et al.[11] reported *in situ* polymerization method for PS/EG nanocomposites. They have discussed about the thermal and electrical properties of nanocomposites. However, much attention was not paid on structural, mechanical (modulus), and dielectric properties of the nanocomposites. Additionally, it was found that presence of EG during *in situ* polymerization changes the molecular weight and distribution of polymer.[11] Moreover, for a similar type of system the percolation threshold depends on the type of processing methods used. For example mechanical mixing, melt mixing, solution mixing, and *in situ* polymerization method have

**Present address:* Department of Metallurgy and Materials Science, College of Engineering, Shivaji Nagar, Pune 411 005, India.
Correspondence to: R. K. Goyal (rkgoyal72@yahoo.co.in or rkg@meta.coep.org.in).

different percolation threshold for EG dispersed polymer nanocomposites.[4]

To our knowledge, there is no detailed discussion about dielectric constant, loss tangent, and modulus of the PS/EG nanocomposites in the literature. Nevertheless, both dielectric constant and loss tangent contribute to the improvement of EMI shielding efficiency. Moreover, higher modulus is required to avoid the warping of the substrate. Therefore, PS/EG nanocomposites were fabricated for the first time using industrial cost effective and simple method, i.e., by dispersing commercial EG in PS via solution method, followed by hot pressing of the mixture. The present work demonstrates a systematic investigation on the morphology, structural, thermal, dynamic modulus, electrical conductivity, and dielectric properties of the PS/EG nanocomposites.

EXPERIMENTAL

Materials

The EG powder and PS granules were obtained from International Advanced Research Center for Powder Metallurgy and New Materials (ARCI), Hyderabad (India), and M/s Reliance Industry (Mumbai, India), India, respectively. Toluene (Laboratory grade) was purchased from Central Drug House Fine Chemicals (Mumbai, India). The PS, EG, and toluene were used as received.

Preparation of polymer nanocomposites

The appropriate quantity of EG powder was dispersed in toluene for 6 h using ultrasonic bath. During processing, ultrasonic waves generated by quartz crystal contributes to separation of graphite particles from their agglomerates. Similarly, PS was dissolved separately in toluene. Both the solutions were mixed together in a beaker and mechanically stirred at 400 rpm for 3 h to get homogeneous mixture. After the complete homogenization of mixture, the beaker was taken out and the solution was poured on glass plate to cast a film. The film was dried initially at room temperature followed by drying in vacuum oven at 100°C for 2 h. The weighed amount of film was placed in the die for hot pressing. The load was applied gradually during heating and maintained at a constant pressure of 30 MPa at 160°C for 5 min. Finally, the samples were cooled naturally to a temperature below the glass transition temperature of PS and ejected out from the die.

Characterization

Thermogravimetric analysis

The thermal stability of the PS and its nanocomposites was determined on a thermogravimetric analysis (TGA, Mettler-Toledo 851e) in nitrogen atmosphere. The samples were heated from 50 to 600°C at a heating rate of 10°C/min. The decomposition temperature of 10% weight loss was denoted by T_{10}. The maximum decomposition temperature (T_{max}) was taken as the temperature corresponding to the maximum of the peak obtained by the first order derivative curve. The % char yield was determined at 600°C.

X-ray diffraction

X-ray diffraction (XRD) pattern of pure EG, PS, and nanocomposites was recorded on Philips X'Pert Analytical PW 3040/60. Ni-filtered CuK_α radiation ($\lambda = 1.54$ Å) generated at 40 kV and 30 mA was used for the angle (2θ) ranged from 15 to 50°. The scan step size and time per step was 0.02° and 5 s, respectively.

Fourier Transform infrared spectroscopy

The Fourier Transform Infrared (FTIR) spectra of EG, PS, and nanocomposite were recorded on Perkin–Elmer FTIR spectrometer (SPECTRUM 2000) in increment of 4 cm^{-1}. The scanning range was from 4000 to 370 cm^{-1}.

Scanning electron microscopy

Morphological analysis of the EG powder and nanocomposite sample was conducted with a scanning electron microscopy (SEM, Philips, XL-30). For this, EG powder was dispersed in an ethanol under ultrasonic bath for 15 min followed by dispersing solution on metal stub. The nanocomposite sample was fractured in liquid nitrogen. Then, the samples were coated with a thin layer of gold using gold sputter coater [Polaron SC 7610] to make the sample electrically conducting.

Dynamic mechanical analysis

The dynamic modulus of the nanocomposites was determined on a DMA (Perkin–Elmer DMA 7e) during the temperature range of 30 to 100°C at an oscillating frequency and heating rate of 1 Hz and 5°C/min, respectively. The static load of 110 mN and dynamic load of 100 mN were applied. The three-point bending mode with bending aspect ratio of ~ 20 was used under argon atmosphere.

Electrical conductivity measurements

The electrical conductivity of the nanocomposites was measured at 30°C by using Keithley high resistivity meter (Model: 6517 A). The hot pressed

TABLE I
Thermal Stability of EG and Nanocomposites

Sample code	EG content in PS by wt %	EG content in PS by vol %	T_{10} (°C)	T_{max} (°C)	Char yield (%)
Pure EG	–	–	–	252	94.65
Pure PS	0	0	384	417	0
PSEG-3	3	1.5	388	420	3.13
PSEG-5	5	2.5	390	419	4.73

sample having 25 mm diameter and 0.5 mm thickness was used for testing.

Dielectric constant

The dielectric constant was determined using an impedance analyzer [HP 4192A, Japan] in a frequency range from 10 KHz to 13 MHz at 30°C. The dielectric constant of the sample was calculated by using eq. (1):

$$\varepsilon = Ct/(\varepsilon_0 A) \quad (1)$$

where C, ε, A, and t are the capacitance, dielectric constant, surface area, and thickness of the dielectric material, respectively. The ε_0 is the permittivity of the free space (8.854×10^{-12} F/m). The dielectric loss tangent is obtained directly from the instrument. Silver conductive paste was applied on both sides of the sample to make good electrical contact with the electrodes.

RESULTS AND DISCUSSIONS

PS nanocomposites filled with varying weight fraction of EG were prepared by solution mixing method followed by hot pressing. The resultant nanocomposites were characterized and discussed in detail in this section. Table I shows the wt % and vol % of the EG added into the PS matrix. From the given weight fraction of EG, the volume fraction of EG can be determined by using eq. (2).

$$V_f = W_f / \left[W_f + (1 - W_f)\rho_f/\rho_m \right] \quad (2)$$

where W_f is the weight fraction of the EG. The density of EG (ρ_f) and PS (ρ_m) was considered 2.2 g/cm^3 and 1.05 g/cm^3, respectively.

Thermogravimetric analysis

The TGA curves of EG, PS, and nanocomposites are shown in Figure 1. It can be seen that EG exhibits very high thermal stability with loss of 5.5 wt % up to 600°C. This may be attributed to the loss of moisture, carboxyl, and hydroxyl groups present in the EG. The addition of EG into PS increased the thermal stability marginally. The T_{10}, for the pure PS (384°C), improved to 388°C and 390°C for the nanocomposites containing 3 wt % and 5 wt % EG, respectively. It can be seen from Table I that there is marginal change in T_{max} for the nanocomposites compared with pure PS. The char yield of the nanocomposites increases from 0 for pure PS to 4.73% for nanocomposite containing 5 wt % EG. A similar trend in char yield was observed for epoxy/graphite platelets.[8] Thus, PS/EG nanocomposites have a better thermal stability compared with that of pure PS. This may be due to the better dispersion and interaction between the EG and PS.

X-ray diffraction

To confirm intercalation of PS into the galleries of EG or change in morphology of PS by the addition of EG, the XRD of nanocomposite was carried out and shown in Figure 2. The d-spacing and 2θ values of EG and nanocomposites are given in Table II. A peak at $2\theta = \sim 26.35°$ corresponding to 002 plane of EG was observed for EG and nanocomposites. Pure PS shows an amorphous hallo between 2θ = 15–25°. XRD shows no significant change in d-spacing and 2θ of 002 peak of EG in the nanocomposites. Moreover, there is not any new diffraction peaks in the nanocomposites. It indicates that neither there is change in morphology of PS or intercalation of PS into the galleries of EG during processing. In other

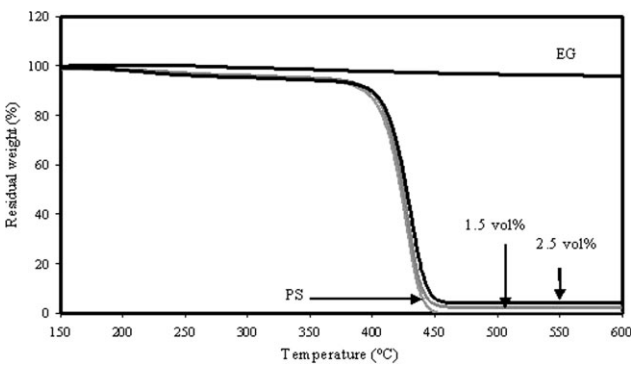

Figure 1 TGA curves of EG, PS, and nanocomposites in nitrogen atmosphere at 10 °C/min.

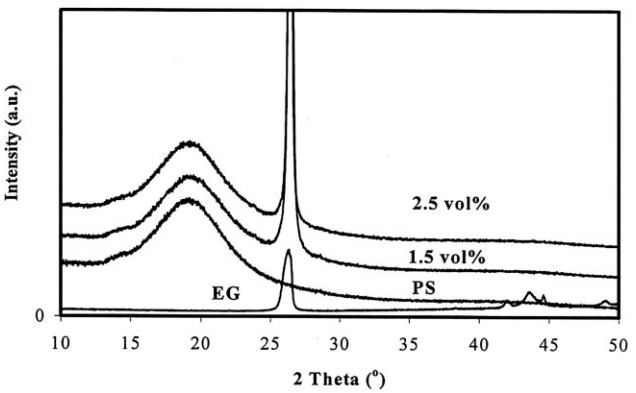

Figure 2 XRD patterns of EG, PS, and nanocomposites.

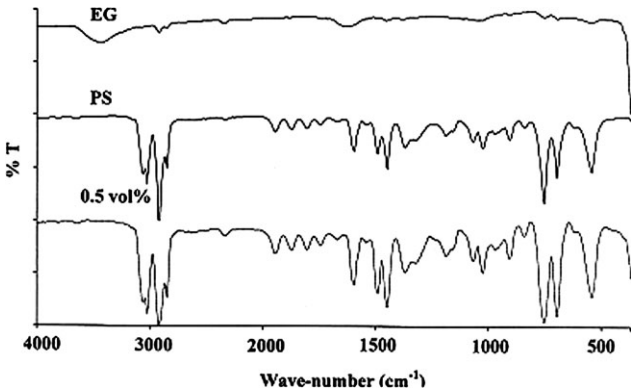

Figure 3 EG(a), PS(b), and 0.5 vol % (c), respectively. FTIR spectra of EG, PS, and nanocomposites.

words, EG particle still consists of a number of carbon layers in nanocomposites.

FTIR spectroscopy

Figure 3 shows the FTIR spectra of EG, PS, and nanocomposites. Figure 3(a) shows the FTIR spectrum of EG. The stretching vibrations of hydroxyl (—OH) group are observed at 3442 and 1377 cm^{-1}. The peak at 1112 cm^{-1} corresponds to the existence of oxygen containing functional groups on the EG surface.[12] Figure 3(b) shows the FTIR spectrum of PS. The absorption bands at 1448, 1492, and 1595 cm^{-1} correspond to aromatic C=C vibration of PS. The peaks at 756 and 699 cm^{-1} correspond to out-of-plane vibration modes of phenyl ring of PS.[13,14] In the spectrum of nanocomposite [Fig. 3(c)], the absorption of EG and PS was found without change or shift in their characteristic bands. This indicates that there is no chemical interaction between the EG and the PS molecules during processing.

Scanning electron microscopy

Figure 4 shows scanning electron microscopy (SEM) micrograph of EG. It can be seen from Figure 4 that EG appears as loose and porous vermicular structure similar to that of reported by Song et al.[15] The width of the graphite sheet is much higher than that of thickness. Hence, the porous structure exhibits higher surface area. Figure 4(b) shows graphite sheet of $\sim$ 1 μm thick, which seems to contain several graphite nanosheets sticking to each other. Figure 5 shows SEM of nanocomposite containing 5 wt % EG. It shows that EG particles are almost uniformly distributed with its three-dimensional network in the matrix. It might be formed due to the penetration of PS into the pores of EG during processing.

TABLE II
Interplaner Spacing (*d*-spacing) and 2θ of EG and Nanocomposites

Sample code	*d*-Spacing (Å)	2θ (°)
EG	3.379	26.35
PSEG-3	3.361	26.52
PSEG-5	3.368	26.47

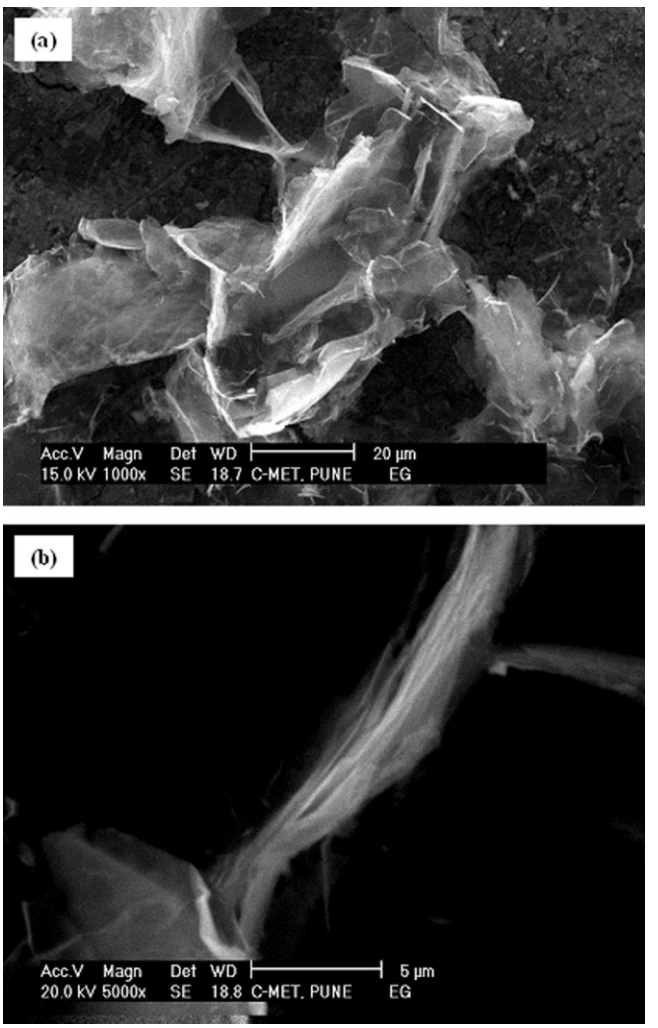

Figure 4 SEM of EG powder at scale bar (a) 20 μm and (b) 5 μm.

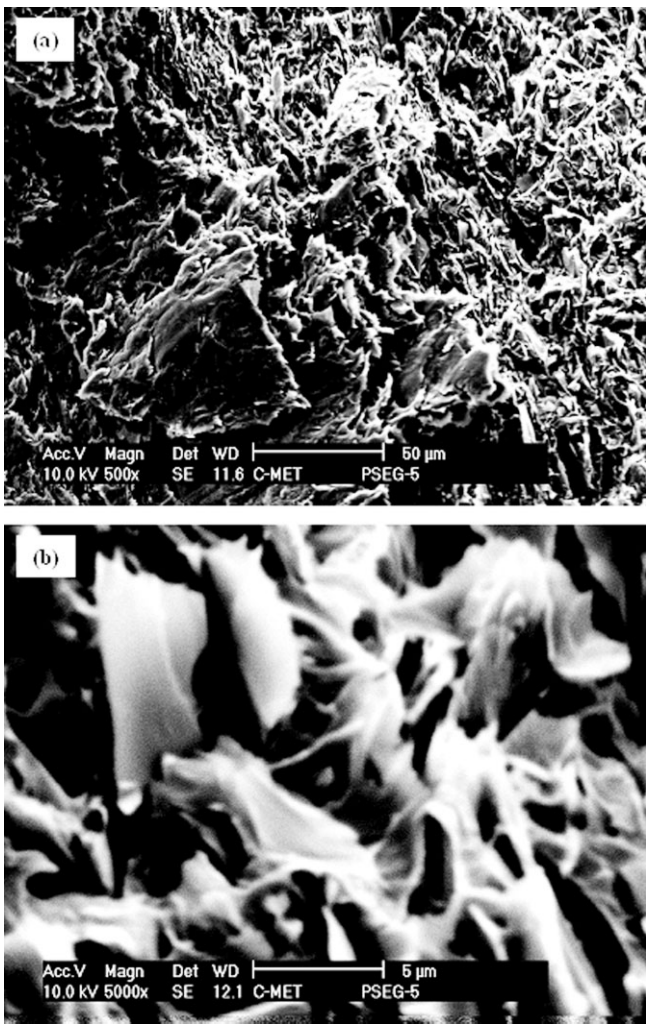

Figure 5 SEM of nanocomposites containing 5 wt % EG at scale bar (a) 50 µm and (b) 5 µm.

Dynamic mechanical analysis

Figure 6(a,b) shows storage modulus of the nanocomposites as a function of temperatures and volume fraction of EG, respectively. It can be seen that storage modulus of PS nanocomposites increases significantly with increasing temperature and EG content. At room temperature, about twofold increase in storage modulus was observed at 5 wt % EG content. This is similar to the results of Krupa et al. reported for the high density polyethylene (HDPE)/graphite composites.[1] However, in present system the improvement in modulus is more significant than that of HDPE/graphite. This is due to the higher modulus of graphite (1 TPa) than that of pure PS and mechanical interlocking between the loose or vermicular structure of EG and PS matrix. The chemical interactions between the EG and PS can be neglected as confirmed from FTIR. Moreover, much higher aspect ratio of EG particles than that of graphite particles results in higher interfacial interaction between the EG and the PS molecules and thus, storage modulus is increased significantly. It is interesting to note that the improvement in modulus of PS filled with 10 wt % (6.25 vol %) multiwall carbon nanotube (MWCNT) is less than twofold.[16] This may probably be due to the lack of interaction between the inner walls of the MWCNT and polymer molecules.

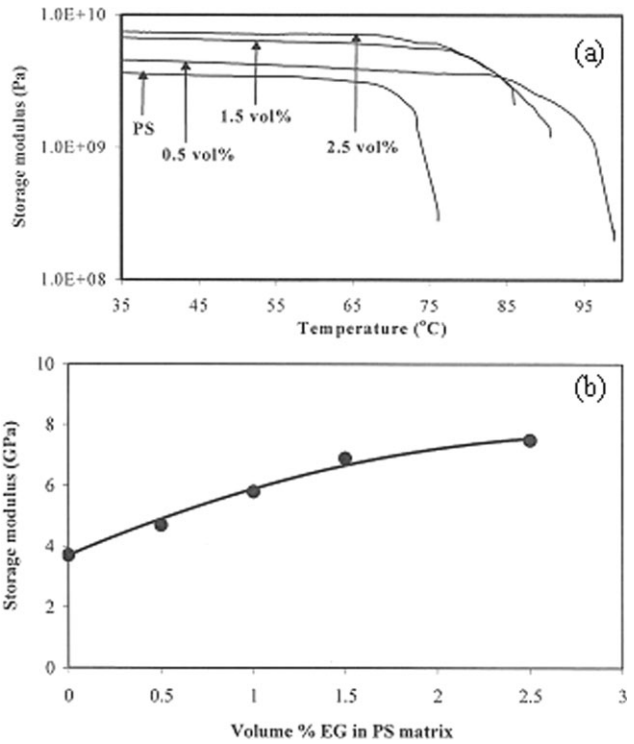

Figure 6 Storage modulus of nanocomposites as a function of (a) temperature and (b) EG in PS matrix.

Electrical conductivity

Figure 7 shows the electrical conductivity of the nanocomposites as a function of EG content. The electrical conductivity of PS is about 1.66×10^{-13} S/cm. As shown in Figure 7, the electrical

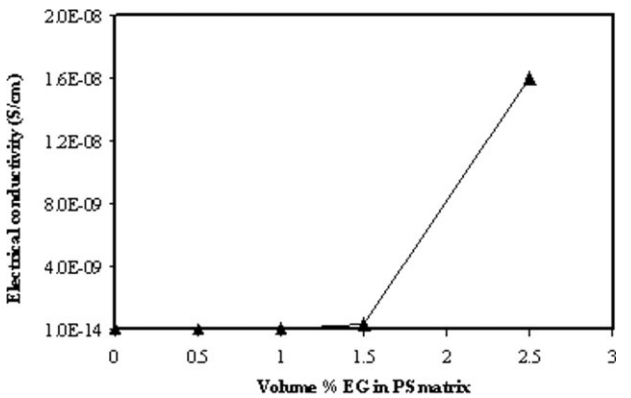

Figure 7 Electrical conductivity of nanocomposites as a function of volume % EG.

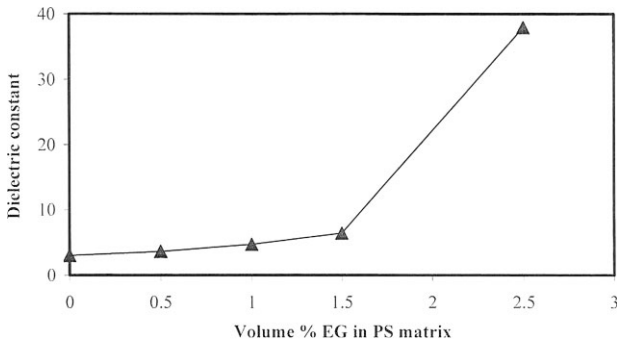

Figure 8 Dielectric constant of nanocomposites as a function of volume % EG.

conductivity of PS increases with increasing EG content. The electrical conductivity of the nanocomposite containing 5 wt % EG is increased to 1.66×10^{-8} S/cm. The result is comparable with the electrical conductivity of polycarbonate/carbon nanofiber (CNF) (6.3 wt %),[17] polyimide/MWCNT (7 wt %),[18] and PS/single-wall carbon nanotube (8.5 wt %)[19] nanocomposites, which were prepared by *in situ* polymerization. Krupa and Chodák[1] reported a percolation threshold value of 12–13 vol % graphite for melt blended PS/graphite composite. In present system, high electrical conductivity of nanocomposite containing 5 wt % (2.5 vol %) EG may be attributed to the enhanced number of conductive paths of EG in the PS matrix.

Dielectric properties

Figure 8 shows the dielectric constant of the nanocomposites as a function of EG at 1 MHz and 30°C. The dielectric constant increases from 3.0 for the pure PS to 37.9 for the nanocomposite containing 2.5 vol % EG. The addition of EG to the PS increases

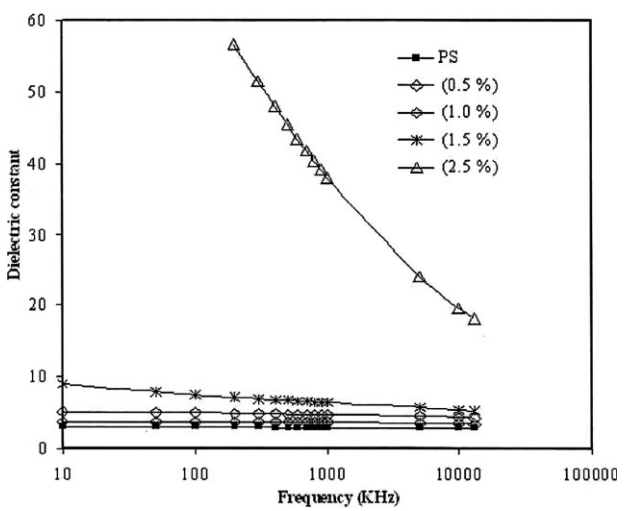

Figure 9 Dielectric constant of nanocomposites as a function of frequency.

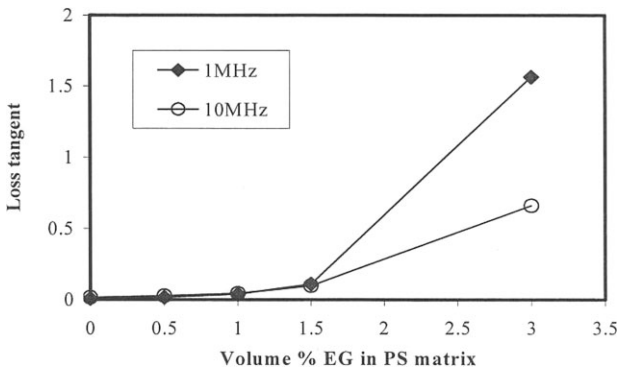

Figure 10 Dielectric loss tangent of nanocomposites as a function of volume % EG.

the dielectric constant due to its higher polarization as compared with pure PS under external field. As the EG content is increased, aggregates of EG particles are formed. The average polarization of the aggregate is higher than that of the individual particles. Hence, the dielectric constant is increased drastically at 2.5 vol % EG. Figure 9 shows the dielectric constant of the nanocomposites as a function of logarithm of frequency at 30°C. It can be seen that the dielectric constant of nanocomposites containing up to 1.5 vol % EG is not affected much as the frequency increases. However, in case of nanocomposite containing 2.5 vol % EG the dielectric constant decreases with increasing frequency. For example, its dielectric constant decreases from 56.5 at 200 KHz to 18.1 at 13 MHz. This is due to the fact that as the frequency is increased, the interfacial dipoles do not have sufficient time to orient themselves in the electric field direction. It is worth noting that dielectric constant of the nanocomposite containing 2.5 vol % EG is higher than that of polyimide/MWCNT (9 wt %).[18] A similar trend in dielectric constant was observed for CNF filled HDPE nanocomposites.[20] Figure 10 shows that as the EG content increases the dielectric loss tangent is increased. The dielectric loss tangent for nanocomposite containing 2.5 vol % EG is about 1.5. The increase in loss tangent might be attributed to the interfacial polarization as reported for other conductor-insulator system. Similar to these results, high dielectric loss tangent was reported for CNF filled HDPE[20] and polyaniline filled fluoroterpolymer.[21] The improvement in both dielectric constant and loss tangent contribute to the improvement in EMI shielding efficiency. Hence, this material may prove to be a cost effective material for the use in EMI shielding applications.

CONCLUSIONS

The cost effective polystyrene/expanded graphite nanocomposites have been successfully prepared by

a simple solvent cast technique followed by hot pressing. The thermal, mechanical, and electrical properties of the nanocomposites are improved significantly. FTIR reveals that there is no chemical interaction between EG and PS molecules. SEM reveals uniform distribution and three-dimensional network of EG in PS matrix. The significant improvement in the storage modulus of nanocomposites has been attributed to the high modulus of EG and mechanical interlocking between the loose or vermicular structure of EG and the PS matrix. The electrical conductivity of the nanocomposites increases with increasing EG content. The dielectric constant and loss tangent of nanocomposites determined at 1 MHz are increased up to 13-fold and 200-fold, respectively.

We are grateful to Dr. T. L. Prakash, Executive Director of C-MET for his active interest in this work. Mr. G. G. Umarji is acknowledged for performing electrical conductivity measurements on samples.

References

1. Krupa, I.; Chodák, I. Eur Polym J 2001, 37, 2159.
2. Luyt, A. S.; Molefi, J. A.; Krump, H. Polym Degrad Stab 2006, 91, 629.
3. Chen, G.; Wu, D.; Weng, W.; Wu, C. Carbon 2003, 41, 619.
4. Zheng, W.; Lu, X.; Wong, S.-C. J Appl Polym Sci 2004, 91, 2781.
5. Wang, W.-P.; Liu, Y.; Li, X.-X.; You, Y.-Z. J Appl Polym Sci 2006, 100, 1427.
6. Chen, G.; Wu, C.; Weng, W.; Wu, D.; Yan, W. Polymer 2003, 44, 1781.
7. Alvarez, M. P.; Poblete, V. H.; Pilleux, M. E.; Fuenzalida, V. M. J Appl Polym Sci 2006, 99, 3005.
8. Yasmin, A.; Daniel, I. M. Polymer 2004, 45, 8211.
9. Chen, G.; Weng, W.; Wu, D.; Wu, C. Eur Polym J 2003, 39, 2329.
10. Pan, Y.-X.; Yu, Z.-Z.; Ou, Y.-C.; Hu, G.-H. J Polym Sci Part B: Polym Phys 2000, 38, 1626.
11. Xiao, M.; Sun, L.; Liu, J.; Li, Y.; Gong, K. Polymer 2002, 43, 2245.
12. Zheng, G.; Wu, J.; Wang, W.; Pan, C. Carbon 2004, 42, 2839.
13. Huo, J. M.; Ko, T. H.; Yang, W.-T.; Lin, J. C.; Jiang, G. J.; Xie, W.; Pan, W. P. J Appl Polym Sci 2004, 91, 101.
14. Wang, H.-W.; Chang, K.-C.; Yeh, J.-M.; Liou, S.-J. J Appl Polym Sci 2004, 91, 1368.
15. Song, L. N.; Xiao, M.; Meng, Y. Z. Compos Sci Technol 2006, 66, 2156.
16. Thostenson, E. T.; Chou, T.-W. J Phys D: Appl Phys 2003, 36, 573.
17. Higgins, B. A.; Brittain, W. J. Eur Polym J 2005, 41, 889.
18. Zhu, B.-K.; Xie, S.-H.; Xu, Z.-K.; Xu, Y.-Y. Compos Sci Tech 2006, 66, 548.
19. Barraza, H. J.; Pomeo, F.; O'Rear, E. A.; Resasco, D. E. Nano Lett 2002, 2, 797.
20. Yang, S.; Benitez, R.; Fuentes, A.; Lozano, K. Compos Sci Technol 2007, 67, 1159.
21. Huang, C.; Zhang, Q. M.; Su, J. Appl Phys Lett 2003, 82, 3502.